

SLAC-PUB-95-6820

Revised

June 1995

Tau Polarization Asymmetry in $B \rightarrow X_s \tau^+ \tau^-$ *

JoAnne L. Hewett

Stanford Linear Accelerator Center, Stanford University, Stanford, CA 94309

Abstract

Rare B decays provide an opportunity to probe for new physics beyond the Standard Model. In this paper, we propose to measure the tau polarization in the inclusive decay $B \rightarrow X_s \tau^+ \tau^-$ and discuss how it can be used, in conjunction with other observables, to completely determine the parameters of the flavor-changing low-energy effective Hamiltonian. Both the Standard Model and several new physics scenarios are examined. This process has a large enough branching fraction, \sim few $\times 10^{-7}$, such that sufficient statistics will eventually be provided by the B-Factories currently under construction.

*Work supported by the Department of Energy, Contract DE-AC03-76SF00515

The recent first observation[1] of the inclusive and exclusive radiative decays $B \rightarrow X_s \gamma$ and $B \rightarrow K^* \gamma$ have placed the study of rare B decays on a new footing. These flavor changing neutral current (FCNC) transitions provide fertile testing ground for the Standard Model (SM) and offer a complementary strategy in the search for new physics by probing the indirect effects of new particles and interactions in higher order processes. In particular, the probing of loop induced couplings can provide a means of testing the detailed structure of the SM at the level of radiative corrections where the Glashow-Iliopoulos-Maiani (GIM) cancellations are important. These first measurements have restricted the magnitude of the electromagnetic penguin transition, resulting in bounds on the value[2] of the ratio of Cabibbo-Kobayashi-Maskawa (CKM) weak mixing matrix elements $|V_{ts}/V_{cb}|$, as well as providing powerful constraints on new physics[3] which in some classes of models complement or surpass the present bounds obtainable from direct collider searches.

The study of rare B decays can be continued with the analysis of the higher order process $B \rightarrow X_s \ell^+ \ell^-$. The experimental situation for these decays is very promising[4], with e^+e^- and hadron colliders closing in on the observation of exclusive modes with $\ell = e$ and μ final states, respectively. These transitions proceed via electromagnetic and Z penguin as well as W box diagrams, and hence can probe different coupling structures than the pure electromagnetic process $B \rightarrow X_s \gamma$. Investigation of this decay mode offers exciting possibilities as various kinematic distributions associated with the final state lepton pair, such as the lepton pair invariant mass spectrum and the lepton pair forward-backward asymmetry, can also be measured in addition to the total rate. These distributions are essential in separating the short distance FCNC processes from the contributing long range physics[5]. In particular, it has been shown[6, 7, 8] that the lepton pair forward-backward asymmetry is sizable for large values of the top-quark mass and is highly sensitive to contributions from new physics. Ali *et al.*[7] have proposed a program to use these distributions, as well as the total

rate for $B \rightarrow X_s \gamma$, to determine the sign and magnitude of each class of short distance FCNC contribution in a model independent fashion. Here, we propose a new observable, the tau polarization asymmetry for the decay $B \rightarrow X_s \tau^+ \tau^-$. We will show that this asymmetry also has a large value for top-quarks in the mass range observed[9] at the Tevatron, and will be measurable with the high statistics available at the B-Factories presently under construction. The tau polarization asymmetry furnishes one more piece of available information for the study of rare B decays. Together with the remaining kinematic distributions mentioned above, the polarization asymmetry (and the $M_{\tau\tau}$ spectrum) will then provide a complete arsenal for a stringent test of the SM.

The transition rate for $B \rightarrow X_s \ell^+ \ell^-$, including QCD corrections[10], is computed via an operator product expansion based on the the effective Hamiltonian,

$$\mathcal{H}_{eff} = \frac{4G_F}{\sqrt{2}} V_{tb} V_{ts}^* \sum_{i=1}^{10} C_i(\mu) \mathcal{O}_i(\mu), \quad (1)$$

which is evolved from the electroweak scale down to $\mu \sim m_b$ by the Renormalization Group Equations. Here V_{ij} represents the relevant CKM factors, and the \mathcal{O}_i are a complete set of renormalized dimension five and six operators involving light fields which govern $b \rightarrow s$ transitions. This basis (involving left-handed fields only) consists of six four-quark operators \mathcal{O}_{1-6} , the electro- and chromo-magnetic operators respectively denoted as $\mathcal{O}_{7,8}$, $\mathcal{O}_9 \sim e \bar{s}_{L\alpha} \gamma_\mu b_{L\alpha} \bar{\ell} \gamma^\mu \ell$, and $\mathcal{O}_{10} \sim e \bar{s}_{L\alpha} \gamma_\mu b_{L\alpha} \bar{\ell} \gamma^\mu \gamma_5 \ell$. For $B \rightarrow X_s \ell^+ \ell^-$, this effective Hamiltonian leads to the matrix element (neglecting the strange quark mass)

$$M = \frac{\sqrt{2}G_F \alpha}{\pi} V_{tb} V_{ts}^* \left[C_9^{eff} \bar{s}_L \gamma_\mu b_L \bar{\ell} \gamma^\mu \ell + C_{10} \bar{s}_L \gamma_\mu b_L \bar{\ell} \gamma^\mu \gamma_5 \ell - 2C_7 m_b \bar{s}_L i \sigma_{\mu\nu} \frac{q^\nu}{q^2} b_R \bar{\ell} \gamma^\mu \ell \right], \quad (2)$$

where q^2 is the momentum transferred to the lepton pair. The Wilson coefficients C_i of the $b \rightarrow s$ operators are evaluated perturbatively at the electroweak scale where the matching

conditions are imposed and are then evolved down to the renormalization scale μ . $C_{7-10}(M_W)$ are given by the Inami-Lim functions[11], $C_2(M_W) = -1$, and $C_{1,3-6}(M_W) = 0$. The expressions for the QCD-renormalized coefficients $C_i(\mu)$ are given explicitly in Refs. [7, 10]. The effective coefficient of \mathcal{O}_9 is defined by $C_9^{eff}(\mu) \equiv C_9(\mu) + Y(\mu, q^2)$ where the function Y contains the contributions from the one-loop matrix element of the four-quark operators and can be found in Refs. [7, 10]. We note that $Y(\mu, q^2)$ contains both real and imaginary contributions (the imaginary piece arises when the c-quarks in the loop are on-shell). The differential branching fraction for $B \rightarrow X_s \tau^+ \tau^-$ is then

$$\begin{aligned} \frac{dB(B \rightarrow X_s \tau^+ \tau^-)}{d\hat{s}} = & B(B \rightarrow X \ell \bar{\nu}) \frac{\alpha^2}{4\pi^2} \frac{|V_{tb} V_{ts}^*|^2}{|V_{cb}|^2} \frac{(1 - \hat{s})^2}{f(z)\kappa(z)} \left[1 - \frac{4x}{\hat{s}} \right]^{1/2} \left\{ \left[|C_9^{eff}|^2 - |C_{10}|^2 \right] 6x \right. \\ & + \left[|C_9^{eff}|^2 + |C_{10}|^2 \right] \left[(\hat{s} - 4x) + (1 + \frac{2x}{\hat{s}})(1 + \hat{s}) \right] \\ & \left. + 12C_7 \mathcal{R}e C_9^{eff} (1 + \frac{2x}{\hat{s}}) + \frac{4|C_7|^2}{\hat{s}} (1 + \frac{2x}{\hat{s}})(2 + \hat{s}) \right\}, \end{aligned} \quad (3)$$

with all Wilson coefficients evaluated at $\mu \sim m_b$, $\hat{s} \equiv q^2/m_b^2$, $x \equiv m_\tau^2/m_b^2$, $z \equiv m_c/m_b$, and $f(z)$ and $\kappa(z)$ represent the phase space and QCD corrections[12], respectively, to the semi-leptonic rate. This agrees with the literature in the zero lepton mass limit. The differential branching fraction is scaled to that of the semi-leptonic decay $B \rightarrow X \ell \nu$ to remove the uncertainties associated with the overall factor of m_b^5 and to reduce the ambiguities involved with the imprecisely determined CKM factors. It is well known that there are large uncertainties (up to $\pm 30\%$) associated with the values of the coefficients $C_{7,9}(\mu)$ due to the renormalization scale dependence of the QCD corrections at leading-logarithmic order, as well as from the scale parameter in α_s . However, this dependence is expected to be reduced at the next-to-leading order. This has recently been demonstrated by Buras and Münz[10] for the case of $C_9(\mu)$, which was found to deviate by only $\pm 8\%$ as the renormalization scale

μ and the QCD scale parameter $\Lambda_{\overline{MS}}$ were varied within their full range of values. The situation for $C_7(\mu)$ differs, however, as only partial NLO calculations exist. These partial calculations do exhibit a reduced μ dependence, and we eagerly await the completion of the NLO computations in this case.

$B \rightarrow X_s \ell^+ \ell^-$ also receives large long distance contributions from the tree-level processes $B \rightarrow K^{(*)} \psi^{(*)}$ followed by $\psi^{(*)} \rightarrow \ell^+ \ell^-$. These pole contributions are incorporated into the lepton pair invariant mass spectrum following the prescription in Ref. [5], where both on- and off-shell vector mesons are considered by employing a Breit-Wigner form for the resonance propagator. This produces an additional contribution to C_9^{eff} of the form

$$\frac{-3\pi}{\alpha^2 m_b^2} \sum_{V_i=\psi,\psi'} \frac{M_{V_i} \Gamma(V_i \rightarrow \ell^+ \ell^-)}{(\hat{s} - M_{V_i}^2/m_b^2) + i\Gamma_{V_i} M_{V_i}/m_b^2}. \quad (4)$$

The relative sign between the short and long distance terms was once a source of controversy, but can be explicitly determined via the analyses presented in Ref. [13]. The resulting differential branching fraction for $B \rightarrow X_s \ell^+ \ell^-$, with and without the long distance resonance contributions, is presented in Fig. 1a for both $\ell = e$ and τ , taking $m_t = 180$ GeV, $m_b = 4.87$ GeV, and $z = 0.316$. We see that the pole contributions clearly overwhelm the branching fraction near the ψ and ψ' peaks, and that there is significant interference between the dispersive part of the resonance and the short distance contributions. However, suitable $\ell^+ \ell^-$ invariant mass cuts can eliminate the resonance contributions, and observations away from these peaks cleanly separate out the short distance physics. This divides the spectrum into two distinct regions[7], (i) low-dilepton mass, $4x \leq \hat{s} \leq M_\psi^2/m_b^2 - \delta$, and (ii) high-dilepton mass, $M_{\psi'}^2/m_b^2 + \delta \leq \hat{s} \leq \hat{s}_{max}$, where δ is to be matched to an experimental cut. The integrated branching fractions (without the pole contributions) for $\ell = e, \mu, \tau$ are presented in Table 1 for both the total and high dilepton mass regions of \hat{s} . We note that the branching

ℓ	$4x \leq \hat{s} \leq 1$	$0.6 \leq \hat{s} \leq 1$
e	1.2×10^{-5}	8.5×10^{-7}
μ	1.0×10^{-5}	8.5×10^{-7}
τ	5.4×10^{-7}	4.3×10^{-7}

Table 1: Integrated branching fractions for $B \rightarrow X_s \ell^+ \ell^-$ for the total and high dilepton mass regions.

fraction for $B \rightarrow X_s \tau^+ \tau^-$ is comparable to that for $\ell = e, \mu$ in the clean \hat{s} region above the ψ' resonance. The exclusive decay $B \rightarrow K \tau^+ \tau^-$ has been computed via heavy meson chiral perturbation theory by Du *et al.*[14], where the exclusive branching fraction was found to be $\sim 50 - 60\%$ of the inclusive; this places $B(B \rightarrow K \tau^+ \tau^-)$ in the range $\sim 2 \times 10^{-7}$. Of course, calculations of exclusive decay rates are inherently model dependent[15], implying that some degree of uncertainty is associated with this result. However, chiral perturbation theory is known to be reliable at energy scales smaller than the typical scale of chiral symmetry breaking, $\Lambda_{CSB} \simeq 4\pi f_\pi/\sqrt{2}$. In $B \rightarrow K \tau^+ \tau^-$, the maximum energy of the K meson in the B rest frame is $(m_B^2 + m_K^2 - 4m_\tau^2)/2m_B \sim 1.5$ GeV, which places most of the available phase space at or comfortably below the scale Λ_{CSB} . We thus expect this method to give a reasonable estimate of the exclusive rate.

The tau polarization asymmetry is defined as

$$P_\tau(\hat{s}) \equiv \frac{dB_{\lambda=-1} - dB_{\lambda=+1}}{dB_{\lambda=-1} + dB_{\lambda=+1}}, \quad (5)$$

where dB represents the differential $B \rightarrow X_s \tau^+ \tau^-$ branching fraction. The spin projection operator is represented as $(1 + \gamma_5 \cdot \hat{s})/2$, with the normalized dot product being defined as $\hat{s} \cdot \hat{p} = \lambda = \pm 1$ with the $- (+)$ sign corresponding to the case where the spin polarization is anti-parallel (parallel) to the direction of the τ^- momentum. This corresponds to the usual definition of a polarization asymmetry, given in terms of couplings, *i.e.*, $(L - R)/(L + R)$,

in the massless case. We note that, of course (and unfortunately), the polarization of final state massless leptons cannot be determined in a collider environment. For the process $B \rightarrow X_s \tau^+ \tau^-$ this asymmetry is then calculated to be

$$P_\tau(\hat{s}) = \frac{-2 [1 - 4x/\hat{s}]^{1/2} C_{10} [\mathcal{R}e C_9^{eff} (1 + 2\hat{s}) + 6C_7]}{D}, \quad (6)$$

where D is given by the expression in the curly brackets in Eq. (3). The tau polarization asymmetry is displayed as a function of $\hat{s} = q^2/m_b^2$ in Fig. 1b, with and without the long distance resonance contributions, and taking $m_t = 180$ GeV. We see that the asymmetry vanishes at threshold and grows with increasing \hat{s} . The value of the total integrated asymmetry (*i.e.*, averaged over the high dilepton mass region, $\hat{s} \geq 0.6$) is -0.484 . The experimentally relevant number of events required to measure an asymmetry a at the $n\sigma$ level is $N = n^2/Ba^2$, and is given here by $N = n^2/(4.3 \times 10^{-7})(-0.484)^2 = (n^2)9.9 \times 10^6$ for the inclusive decay. The exclusive case of $B \rightarrow K\tau^+ \tau^-$ would then yield $N \sim (n^2)2.1 \times 10^7$. This result demonstrates that P_τ should be accessible, after several years of running (even when τ identification efficiencies are taken into account), at the B-Factories under construction.

The formalism for determining the polarization of τ 's has been extensively studied[16] for many years (in fact, even before the tau was discovered!). More recently, polarization measurements of final state τ leptons have been proposed as a useful tool in discerning physics beyond the SM in a variety of processes. Some examples include, determining the transverse and longitudinal τ polarization in $B, \Lambda_b \rightarrow X\tau\nu$ [17], τ polarization asymmetry at hadron colliders as a probe of new Z' couplings[18], using τ polarization to enhance charged Higgs boson searches at hadron colliders[19], probing neutralino mixing through τ polarization in scalar τ decay[20], and in searching for CP violation in the leptonic sector[21]. These measurements can take place as information on the tau's polarization state is carried to its decay

products. In particular, the momentum distribution of the decay products A (in $\tau \rightarrow A\nu_\tau$, where $A = e\bar{\nu}_e, \mu\bar{\nu}_\mu, n\pi, \rho, a_1, \dots$) has a large dependence on the spin polarization state of the parent τ lepton. This dependence is sufficiently striking, such that the tau's helicity may be established from a relatively low number of events[16]. The formalism developed for determining the tau's spin polarization on the Z resonance can be applied in this case in the $\tau^+\tau^-$ invariant mass rest frame, except that one cannot take the collinear limit $E_\tau \gg m_\tau$. The resulting decay distributions cannot, however, be measured in this rest frame due to the two undetected neutrinos, and one is forced to transform to the laboratory frame to implement this procedure. As an example of how accurately the tau's polarization can be determined, we note that the four LEP detectors have made separate polarization measurements[22] in each of the τ decay modes $e\nu\bar{\nu}, \mu\nu\bar{\nu}, \pi(K)\nu, \rho\nu$, and $a_1\nu$ (in addition, DELPHI has used an inclusive one-prong hadronic analysis). These modes account for $\sim 80\%$ of all τ decays. The tau polarization has then been determined with an overall error of $10 - 15\%$ per experiment. If B-factory experiments can achieve similar results (and there is no reason to believe otherwise) then they will have sufficient statistics to measure the asymmetry P_τ .

We now explore the sensitivity of P_τ to new physics. We first investigate the influence of a change in sign of the short distance contributions to C_{7-10} (holding the magnitudes constant). The results are shown in Fig. 2a, where the dashed, dash-dotted, dotted, solid, and long-dashed curves represent the polarization asymmetry with $C_{10}(M_W) \rightarrow -C_{10}(M_W)$, $C_{9,10}(M_W) \rightarrow -C_{9,10}(M_W)$, $C_9(M_W) \rightarrow -C_9(M_W)$, the SM, and $C_{7,8}(M_W) \rightarrow -C_{7,8}(M_W)$, respectively. We see that there is large sensitivity to any combination of sign changes in $C_{9,10}(M_W)$, but little variation to a sign change in the electro- and chromomagnetic operator coefficients. This is due to the fact that the operators $\mathcal{O}_{9,10}$ dominate the decay in the high \hat{s} region. We next examine P_τ in two-Higgs-Doublet models of type II, where a charged Higgs boson participates in the decay via virtual exchange in the γ, Z

penguin and box diagrams. The modifications to the Wilson coefficients in this model are given in Deshpande *et al.*[23]. The resulting tau polarization asymmetry (with $\hat{s} = 0.7$ and $m_t = 180 \text{ GeV}$) for various values of the charged Higgs mass is presented in Fig. 2b as a function of $\tan\beta \equiv v_2/v_1$, the ratio of vacuum expectation values of the two doublets. We see that the effect of the H^\pm is negligible for values of the parameters which are consistent with the present constraints from $B \rightarrow X_s \gamma$ [1, 24], *i.e.*, $\tan\beta \gtrsim 1$ and $m_{H^\pm} \gtrsim 240 \text{ GeV}$. Finally, we study the effects of anomalous trilinear gauge boson couplings in $B \rightarrow X_s \ell^+ \ell^-$. The dependence of the $C_i(M_W)$ on these anomalous couplings can be found in Ref. [25]. Figure 2c displays the deviation of P_τ (for $\hat{s} = 0.7$ and $m_t = 180 \text{ GeV}$) with non-vanishing values of the anomalous magnetic dipole and electric quadrupole $WW\gamma$ coupling parameters, $\Delta\kappa_\gamma$ and λ_γ , respectively, and of the parameter g_5^Z which governs the term $ig_5^Z \epsilon^{\mu\nu\lambda\rho} (W_\mu^\dagger \partial_\lambda W_\nu - W_\nu \partial_\lambda W_\mu^\dagger) Z_\rho$ in the WWZ Lagrangian. For the anomalous coupling parameters considered here, $B \rightarrow X_s \ell^+ \ell^-$ naturally avoids the problem of introducing cutoffs to regulate the divergent loop integrals due to cancellations provided by the GIM mechanism[25]. As expected, we find little sensitivity to modifications in $C_{7,8}(M_W)$ from anomalous $WW\gamma$ couplings, but a large variation due to the influence of anomalous WWZ vertices in $C_{9,10}(M_W)$.

In order to ascertain how much quantitative information is obtainable on the values of the Wilson coefficients $C_{7,9,10}$ from the various kinematic distributions, we perform a Monte Carlo study. For illustration purposes, we will examine the case where the SM situation is realized, *i.e.*, we assume that there is no new physics contributing to these decays. For the process $B \rightarrow X_s \ell^+ \ell^-$, we consider the $M_{\ell^+\ell^-}$ distribution and the lepton pair forward-backward asymmetry[26] for $\ell = e, \mu$, and τ , as well as the tau polarization asymmetry. We take the lepton pair invariant mass spectrum and divide it into 9 bins. These bins are distributed as follows: 6 bins of equal size, $\Delta\hat{s} = 0.05$, are taken in the low dilepton mass

region below the J/ψ resonance, $0.02 \leq \hat{s} \leq 0.32$ (where we have also cut out the region near zero due to the photon pole), and 3 bins in the high dilepton mass region above the ψ' pole, which are taken to be $0.6 \leq \hat{s} \leq 0.7$, $0.7 \leq \hat{s} \leq 0.8$, and $0.8 \leq \hat{s} \leq 1.0$. The number of events per bin is given by

$$N_{\text{bin}} = \mathcal{L} \int_{\hat{s}_{\text{min}}}^{\hat{s}_{\text{max}}} \frac{d\Gamma}{d\hat{s}} \hat{s}, \quad (7)$$

and the average value of the asymmetries in each bin is then

$$\langle A \rangle_{\text{bin}} = \frac{\mathcal{L}}{N_{\text{bin}}} \int_{\hat{s}_{\text{min}}}^{\hat{s}_{\text{max}}} A \frac{d\Gamma}{d\hat{s}} \hat{s}. \quad (8)$$

We also include in our study the inclusive decay $B \rightarrow X_s \gamma$, which is directly proportional to $|C_7(\mu)|^2$. For this case we only consider the total rate. Next we generate “data” (assuming the SM is correct) for an integrated luminosity of $5 \times 10^8 B\bar{B}$ pairs; this corresponds to the expected total luminosity after several years of running at future B-factories. The “data” is then statistically fluctuated by a normalized Gaussian distributed random number procedure. The statistical errors are taken to be $\delta N = \sqrt{N}$ and $\delta A = \sqrt{(1 - A^2)/N}$. We include statistical errors only for the decay $B \rightarrow X_s \ell^+ \ell^-$, as even for this large value of integrated luminosity we expect the errors in each bin to be statistically dominated. The situation differs for $B \rightarrow X_s \gamma$, however, as the statistical precision will far exceed the possible systematic (and theoretical) accuracy. Hence, in this case we assume a flat 10% error in the measurement of the branching fraction. We then perform a three dimensional χ^2 fit to the coefficients $C_{7,9,10}(\mu)$ from the “data” according to the usual prescription

$$\chi_i^2 = \sum_{\text{bins}} \left(\frac{Q_i^{\text{obs}} - Q_i^{\text{SM}}}{\delta Q_i} \right)^2, \quad (9)$$

where $Q_i^{\text{obs,SM}}$, δQ_i represent the “data”, the SM expectations, and the error for each observable quantity Q_i . The resulting 95% C.L. allowed regions as projected onto the $C_9(\mu) - C_{10}(\mu)$

and $C_7(\mu) - C_{10}(\mu)$ planes are presented in Fig. 3a and b, respectively. In these figures, the point ‘S’ labels the SM expectations (assuming $m_t = 180$ GeV), and the diamond represents the best fit value which has a total $\chi^2 = 24.6/25$ dof. We see that the determined ranges for the coefficients encompasses their SM values. The 95% C.L. ranges for the coefficients are found to be $C_7(\mu) = 0.3208^{+0.0286}_{-0.0268}$, $C_9(\mu) = -2.300^{+0.425}_{-0.495}$, and $C_{10}(\mu) = 4.834^{+0.478}_{-0.500}$, corresponding to a 7.5%, 20% and 10% determination of C_7 , C_9 , and C_{10} , respectively. Clearly, the values extracted for C_9 and C_{10} are highly correlated, but this is not the case for C_7 and C_{10} . If we take $C_7(\mu)$ to have opposite sign, *i.e.*, $C_7(\mu) = -|C_7(\mu)|$, we find that the fit is quite poor with the best fit yielding $\chi^2 = 539.1/25$ dof.

In conclusion, we have shown that measurement of the τ polarization in $B \rightarrow X_s \tau^+ \tau^-$ is highly sensitive to new physics and hence provides a powerful probe of the SM. Together, measurement of the polarization asymmetry and the remaining kinematic distributions associated with $B \rightarrow X_s \ell^+ \ell^-$, will provide enough information to completely determine the parameters of the FCNC effective Hamiltonian. We find that the values of the polarization can be precisely determined with the large data samples that will be available at the B-Factories presently under construction. We eagerly await the completion of these machines!

ACKNOWLEDGEMENTS

The author thanks T.G. Rizzo for invaluable discussions, and the Phenomenology Institute at the University of Wisconsin for their hospitality while this work was completed.

References

- [1] M.S. Alam *et al.*, (CLEO Collaboration), Phys. Rev. Lett. **74**, 2885 (1995); R. Ammar *et al.*, (CLEO Collaboration), Phys. Rev. Lett. **71**, 674 (1993).
- [2] A. Ali and C. Greub, Z. Phys. **C60**, 433 (1993).
- [3] For a review see, J.L. Hewett, in *Proceedings of the 21st Annual SLAC Summer Institute*, ed. L. DePorcel and C. Dunwoodie (SLAC-Report-444, Stanford, CA, 1994).
- [4] R. Balest *et al.*, (CLEO Collaboration), to appear in *Proceedings of the 1994 International Conference on High Energy Physics*, Glasgow, Scotland, CLEO-CONF-94-4 (1994); C. Anway-Wiese, (CDF Collaboration), in *Proceedings of the 8th Meeting of the Division of Particles and Fields of the American Physical Society*, Albuquerque, New Mexico, 1994, ed. S. Seidel (World Scientific, Singapore, 1995).
- [5] N.G. Deshpande, J. Trampetic, and K. Panrose, Phys. Rev. **D39**, 1461 (1989); C.S. Lim, T. Morozumi, and A.I. Sanda, Phys. Lett. **B218**, 343 (1989).
- [6] A. Ali, T. Mannel, and T. Morozumi, Phys. Lett. **B273**, 505 (1991).
- [7] A. Ali, G.F. Giudice, and T. Mannel, Z. Phys. **C67**, 417 (1995).
- [8] C. Greub, A. Ioannissian, and D. Wyler, Phys. Lett. **B346**, 149 (1995); D. Liu, Univ. of Tasmania Report (1995); G. Burdman, Fermilab Report Pub-95/113-T (1995).
- [9] F. Abe *et al.*, (CDF Collaboration), Phys. Rev. Lett. **74**, 2626 (1995); S. Abachi *et al.*, (D0 Collaboration), *ibid.*, **74**, 2632 (1995).

[10] N.G. Deshpande and J. Trampetic, Phys. Rev. **D60**, 2583 (1988); B. Grinstein, M.J. Savage, and M.B. Wise, Nucl. Phys. **B319**, 271 (1989); A.J. Buras and M. Münz, Phys. Rev. **D52**, 186 (1995).

[11] T. Inami and C.S. Lim, Prog. Theor. Phys. **65**, 297 (1981).

[12] N. Cabibbo and L. Maiani, Phys. Lett. **79B**, 109 (1978).

[13] P.J. O'Donnell and H.K. Tung, Phys. Rev. **D43**, R2067 (1991); A.I. Vainshtein, V.I. Zakharov, L.B. Okun, and M.A. Shifman, Yad. Fiz. **24**, 820 (1976) [Sov. J. Nucl. Phys. **24**, 427 (1976)]; N.G. Deshpande, X.-G. He, and J. Trampetic, Univ. of Oregon Report OITS-564 (1995).

[14] D. Du, C. Liu, and D. Zhang, Phys. Lett. **B317**, 179 (1993).

[15] For a review, see R. Grigjanis, P.J. O'Donnell, M. Sutherland, and H. Navelet, Phys. Rep. **228**, 93 (1993).

[16] Y.S. Tsai, Phys. Rev. **D4**, 2821 (1971); T. Hagiwara, S.-Y. Pi, and A. Sanda, Ann. Phys. (N.Y.) **106**, 134 (1977); J. Kühn and F. Wagner Nucl. Phys. **B236**, 16 (1984); P. Aurenche and R. Kinnunen, Z. Phys. **C28**, 261 (1985); K. Hagiwara, A.D. Martin, and D. Zeppenfeld, Phys. Lett. **B235**, 198 (1990); A. Rouge, Z. Phys. **C48**, 75 (1990).

[17] A.F. Falk, Z. Ligeti, M. Neubert, Y. Nir, Phys. Lett. **B326**, 145 (1994); Y. Grossman and Z. Ligeti, Phys. Lett. **B347**, 399 (1995); R. Garisto, Phys. Rev. **D51**, 1107 (1995); M. Gremm, G. Köpp, and L.M. Sehgal, Phys. Rev. **D52**, 1588 (1995).

[18] J.D. Anderson, M.H. Austern, and R.N. Cahn, Phys. Rev. Lett. **69**, 25 (1992), and Phys. Rev. **D46**, 290 (1992).

[19] B.K. Bullock, K. Hagiwara, and A.D. Martin, Phys. Rev. Lett. **67**, 3055 (1989); Nucl. Phys. **B395**, 499 (1993); D.P. Roy, Phys. Lett. **B277**, 183 (1992); S. Raychaudhuri and D.P. Roy, Phys. Rev. **D52**, 1556 (1995).

[20] M.N. Nojiri, Phys. Rev. **D51**, 6281 (1995).

[21] Y.S. Tsai, Phys. Rev. **D51**, 3172 (1995).

[22] D. Buskulic *et al.*, (ALEPH Collaboration), CERN Report CERN-PPE/95-023 (1995), and Z. Phys. **C59**, 369 (1993); P. Abreu *et al.*, (DELPHI Collaboration), Z. Phys. **C67**, 183 (1995); M. Acciarri *et al.*, (L3 Collaboration), Phys. Lett. **B341**, 245 (1994); R. Akers *et al.*, (OPAL Collaboration), Z. Phys. **C65**, 1 (1995).

[23] N.G. Deshpande, K. Panrose, and J. Trampetic, Phys. Lett. **B308**, 322 (1993).

[24] J.L. Hewett, Phys. Rev. Lett. **70**, 1045 (1993); V. Barger, M. Berger, and R.J.N. Phillips, Phys. Rev. Lett. **70**, 1368 (1993).

[25] S.-P. Chia, Phys. Lett. **B240**, 465 (1990); K.A. Peterson, Phys. Lett. **B282**, 207 (1992); T.G. Rizzo, Phys. Lett. **B315**, 471 (1993); G. Baillie, Z. Phys. **C61**, 667 (1994).

[26] We note that the expressions given for the lepton pair forward-backward asymmetry in Refs. 6 and 7 do not agree; we have found agreement with that of Ref. 6. In the case of massive leptons, *i.e.*, $\ell = \tau$, one must include an additional overall factor of $[1 - 4x/\hat{s}]^{1/2}$ in the asymmetry.

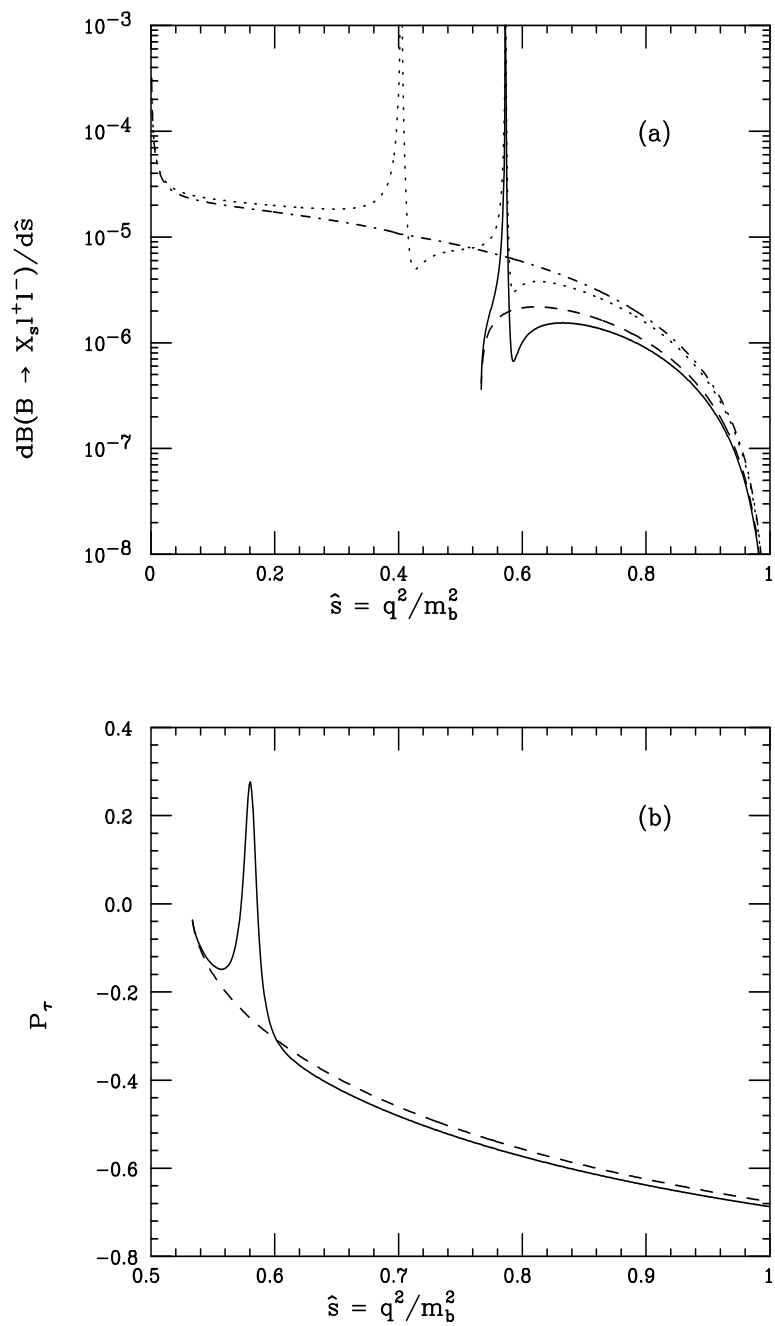


Figure 1: (a) Differential branching fraction and (b) tau polarization asymmetry as a function of \hat{s} for $\ell = \tau$ (solid and dashed curves) and $\ell = e$ (dotted and dash-dotted curves), with and without the long distance resonance contribution.

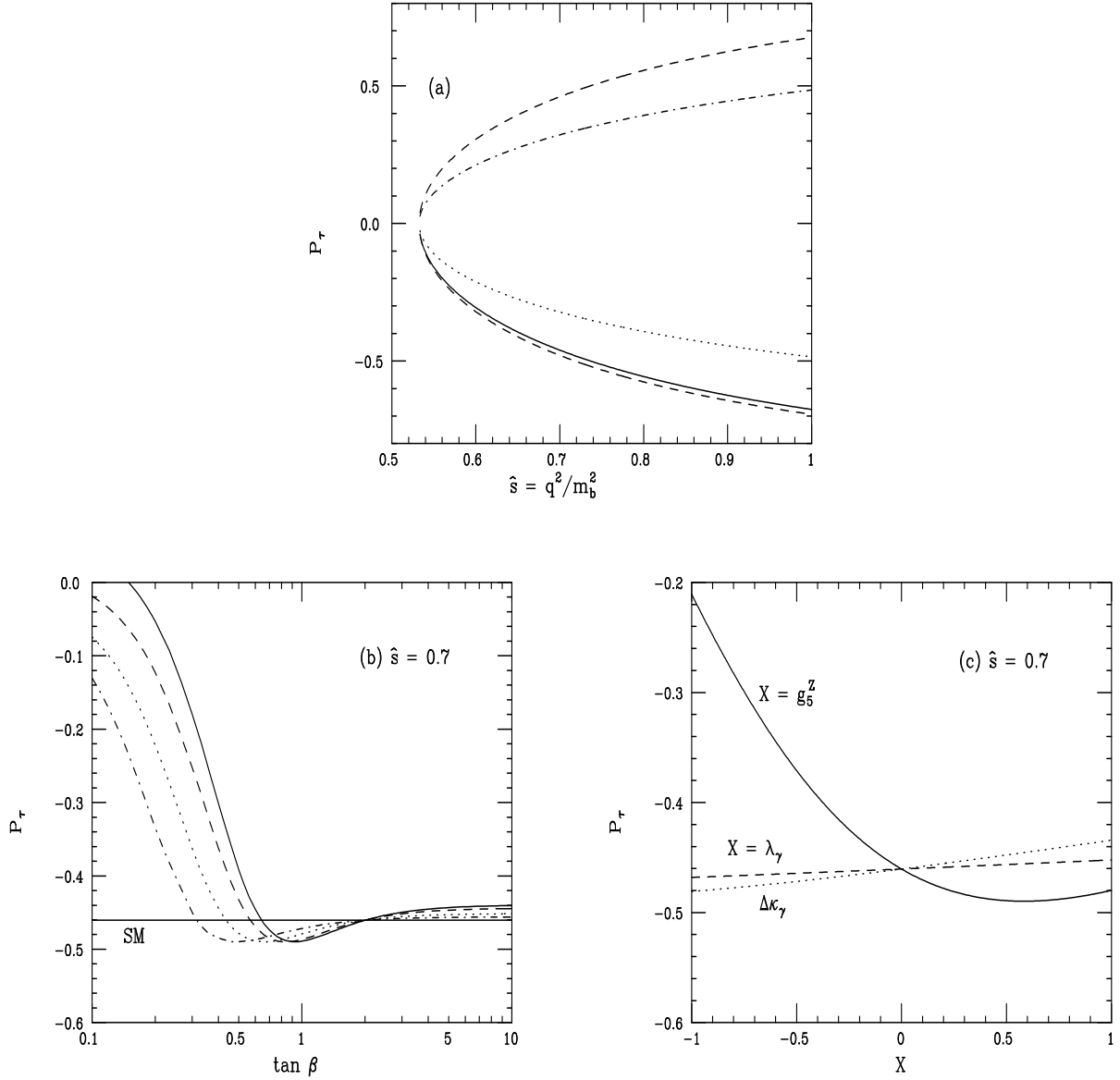


Figure 2: Tau polarization asymmetry (a) with changes in the sign of the Wilson coefficients at the electroweak scale, corresponding to C_{10} , $C_{9,10}$, C_9 , SM $C_{7,8}$ from top to bottom; (b) in two-Higgs-doublet models as a function of $\tan \beta$ with $m_{H^\pm} = 50, 100, 250, 500$ corresponding to the solid, dashed, dotted, and dash-dotted curves, respectively. The SM value is denoted by the solid horizontal line. (c) with anomalous couplings $WW\gamma$ and WWZ couplings as described in the text.

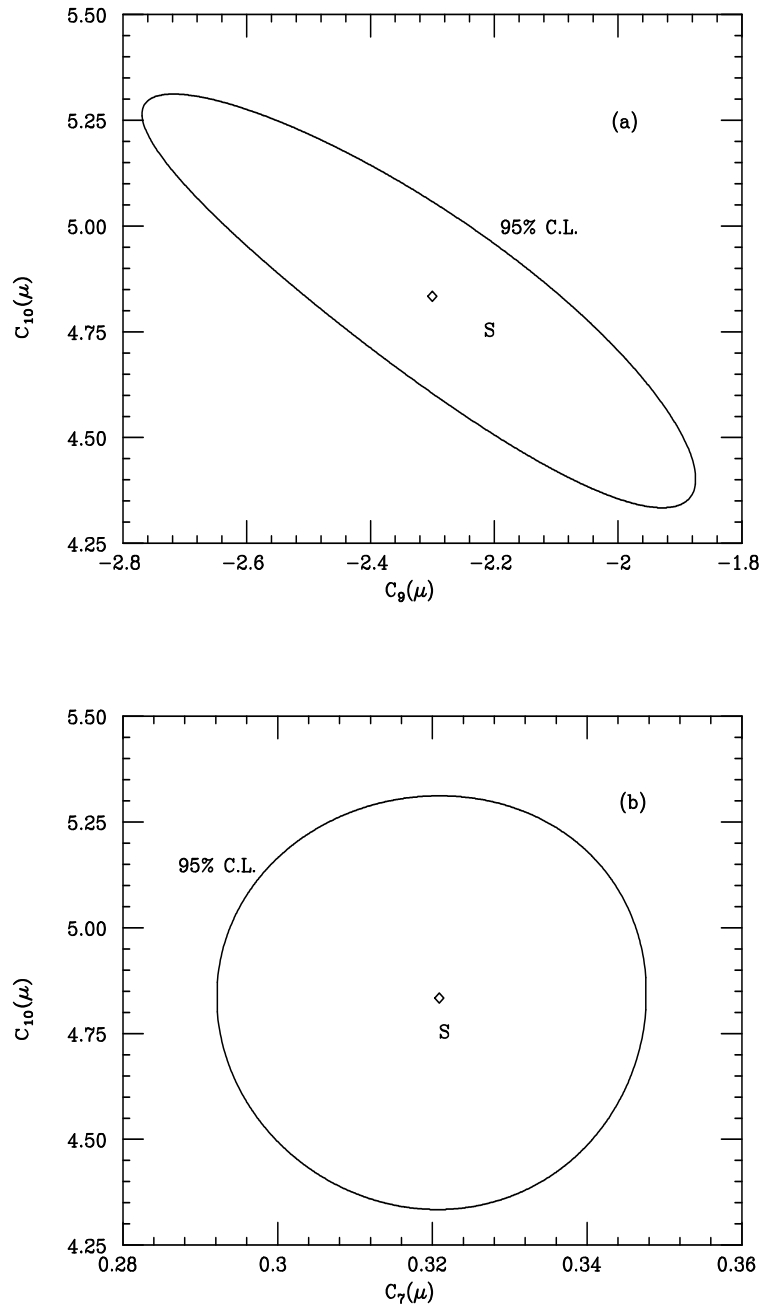


Figure 3: 95% C.L. contour in the (a) $C_9 - C_{10}$, (b) $C_7 - C_{10}$ plane from the fit procedure described in the text. 'S' labels the SM prediction and the diamond represents the best fit values.